

## TWO-DIMENSIONAL BUMPS IN PIECEWISE SMOOTH NEURAL

The simplest example of a one-dimensional (1D) neural field model is the scalar equation [2]

$$(1.1) \quad \frac{u(x, t)}{\tau} = -u(x, t) + \int_{-\infty}^{\infty} w(x - x') f(u(x', t)) dx' + h(x, t).$$

The neural field  $u(x, t)$  represents the local activity of a population of neurons at position  $x$  at time  $t$ ,  $\tau$  is a membrane or synaptic time constant,  $h(x, t)$  represents an external input, and  $w(x)$  is a synaptic weight distribution. We assume that  $w$  is a continuous function satisfying  $w(-x) = w(x)$  and  $\int_{-\infty}^{\infty} w(x) dx < \infty$ . The nonlinearity  $f$  denotes an output firing rate function. A typical choice for  $f$  is a bounded, positive monotonic function such as the sigmoid

$$(1.2) \quad f(u) = \frac{1}{1 + e^{-(u - \theta)}}$$

with gain  $\beta$  and threshold  $\theta$ . Considerable insight into particular classes of spatially localized solutions of (1.1) and various generalizations involving vector-valued fields can be obtained by taking the high-gain limit  $\beta \rightarrow \infty$  such that  $f$  becomes a Heaviside function

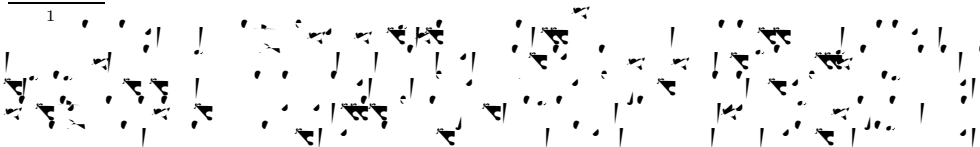
$$(1.3) \quad f(u) = H(u - \theta) = \begin{cases} 0 & \text{if } u < \theta, \\ 1 & \text{if } u > \theta. \end{cases}$$

It is then possible to establish existence of stationary and traveling pulse solutions by explicit construction, and to determine local stability in terms of an associated Evans function by linearizing the neural field equations about the pulse solution [2, 7, 30, 31, 32, 43]. In the case of stationary pulses or bumps, local stability reduces to the problem of calculating the effects of perturbations at the bump boundary, where  $u(x) = \theta$ .

Equation (1.1) was first analyzed in detail by Amari [2], who showed that in the case of a Heaviside function  $H$  and a homogeneous external input  $h$ , the network can support a stable stationary bump solution when the weight distribution  $w(x)$  is given by a so-called Mexican hat function with the following properties:<sup>1</sup>

- (i)  $w(x) > 0$  for  $x \in [0, x_0)$  with  $w(x_0) = 0$ .
- (ii)  $w(x) < 0$  for  $x \in (x_0, \infty)$ .
- (iii)  $w(x)$  is decreasing on  $[0, x_0]$ .
- (iv)  $w(x)$  has a unique minimum on  $\mathbb{R}^+$  at  $x = x_1$  with  $x_1 > x_0$  and  $w(x)$  strictly increasing on  $(x_1, \infty)$ .

On the other hand, in the case of a purely excitatory network with  $w(x)$  a positive, monotonically decreasing function, any bump solution is unstable and tends to break up into a pair of counterpropagating fronts. Following Amari's original analysis, Kishimoto and Amari [23] proved the existence of a stationary pulse for a smooth

<sup>1</sup> 

sigmoidal nonlinearity  $f$ , rather than a Heaviside function, using a fixed point theorem. Moreover, rigorous functional analytical techniques have been used to study the existence and (absolute) stability of stationary bump solutions for a general class of neural field models with smooth  $f$ , where the spatial domain is taken to be bounded rather than infinite [12].

The constructive approach based on the use of Heaviside functions has been generalized in a number of ways (see the review by Coombes [5]). These include more general weight distributions for which multiple bump states can arise [24, 25], inhomogeneous neural fields [18], two-dimensional (2D) bumps [14, 15, 25, 39], and weakly

can be constructed. However, the presence of a Heaviside function in the dynamics of the synaptic depression variable means that the resulting dynamical system is piecewise smooth, which considerably complicates the stability analysis. Indeed, we have recently shown how the local stability of a 1D stationary bump can be formulated in terms of a system of pseudolinear equations that keep track of the sign of perturbations of the bump boundary [21]. Solutions to these equations establish that sufficiently strong synaptic depression can destabilize a bump. In this paper we extend our analysis of piecewise smooth neural fields with synaptic depression to the case of a 2D network. We also give a more detailed derivation of our previous stability results for a 1D network.

## 2. One-dimensional bumps.

**2.1. Existence of one-dimensional bumps.** On setting  $f(u) = H(u - \theta)$ , a stationary solution  $(U(x), Q(x))$  of (1.6) satisfies the pair of equations

$$(2.1) \quad U(x) = \int_{-\infty}^{\infty} Q(x') w(x - x') H(U(x') - \theta) dx',$$

$$(2.2) \quad Q(x) = 1 - \frac{1}{1 + \beta} H(U(x) - \theta).$$

Let  $R[U] = \{x | U(x) > \theta\}$  be the region over which the field is excited or super-threshold. Exploiting the fact that any solution can be arbitrarily translated along the  $x$ -axis, we define a stationary bump solution of half-width  $a$  to be one for which  $R[U] = (-a, a)$ . Substituting (2.2) into (2.1) then yields

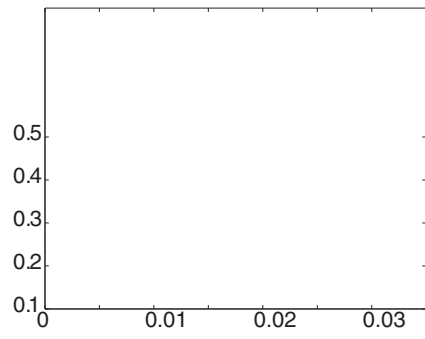
$$(2.3) \quad U(x) = \frac{1}{1 + \beta} [W(x + a) + W(x - a)],$$

where  $W(x) = \int_0^x w(y) dy$ . As a simple example, consider a Mexican hat distribution given by the difference-of-exponentials

$$(2.4) \quad w(|x - x'|) = e^{-|x - x'|} - A e^{-\alpha|x - x'|}.$$

Substituting the weight function (2.4) into the steady-state solution for  $U(x)$  and evaluating the integral yields

$$U(x) = \frac{1}{(1 + \beta)} \left[ \frac{2 \sinh \alpha a e^{-x} - 2A \sinh \alpha a e^{-x}}{2 \sinh \alpha a e^{-x} - 2A \sinh \alpha a e^{-x}} \right], \quad x \in \{ \dots \} \ll$$



Denote the perturbations of the bump boundary by  $\pm(t)$  such that

$$u(a + \Delta_+(t), t) = u(-a + \Delta_-(t), t) =$$

for all  $t > 0$ . Taylor expanding these threshold conditions to first order in  $\Delta$ , we find that

$$(2.8) \quad \pm(t) \approx \pm \frac{(\pm a, t)}{|U'(a)|}.$$

We then introduce the auxiliary field

$$(2.9) \quad (x, t) = \int_{-a + \Delta_-(t)}^{a + \Delta_+(t)} w(x - x') (x', t) dx'.$$

The motivation for this is that a small shift in the location of the bump boundary means that in a small neighborhood of the bump boundary the synaptic depression variable will start to switch its steady-state value from  $q = 1$  to  $q = (1 + \Delta)^{-1}$  or vice-versa according to (1.6b). That is,  $(x, t)$  will undergo  $\mathcal{O}(1/\Delta)$  changes over a timescale of  $\Delta^{-1}$ . However, this doesn't necessarily imply that the bump solution is unstable, since the region over which  $(x, t) = \mathcal{O}(1/\Delta)$  may shrink to zero. This is captured by the dynamics of the auxiliary field  $(x, t)$ , which will remain  $\mathcal{O}(1)$  when  $(x, t)$  is  $\mathcal{O}(1/\Delta)$  over an infinitesimal interval.

Differentiating (2.9) with respect to time shows that

$$\begin{aligned} \frac{(x, t)}{t} = & \int_{-a + \Delta_-(t)}^{a + \Delta_+(t)} w(x - x') \frac{(x', t)}{t} dx' \\ & + w(x - a - \Delta_+(t)) (a + \Delta_+(t), t) \dot{\Delta}_+(t) \\ & - w(x + a - \Delta_-(t)) (-a + \Delta_-(t), t) \dot{\Delta}_-(t), \end{aligned}$$

where  $\dot{\Delta} = d\Delta/dt$ . Substituting for  $\dot{\Delta} / t$  using (2.7) and replacing the final term on the right-hand side of (2.6) by  $\dot{\Delta}_-(t)$  leads to the pair of equations

$$(2.10) \quad \frac{(x, t)}{t} = - (x, t) + (x, t) + \frac{1}{t} \int_{-a + \Delta_-(t)}^{a + \Delta_+(t)} w(x - x') Q(x') dx' - \frac{1}{t} \int_{-a}^a w(x - x') Q(x') dx',$$

$$\begin{aligned} \frac{(x, t)}{t} = & - (x, t) + (x, t) \\ & - \int_{-a + \Delta_-(t)}^{a + \Delta_+(t)} w(x - x') Q(x') H(U(x') + (x', t) - \Delta) dx' \\ & + \int_{-a + \Delta}^{a + \Delta_+(t)} w(x - x') Q(x') H(U(x') + (x', t) - \Delta) dx' \end{aligned}$$





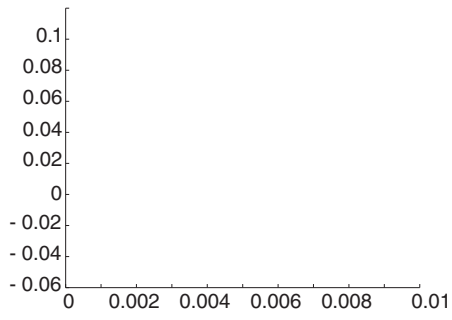




where

$$= \frac{w(0) + w(2a)}$$





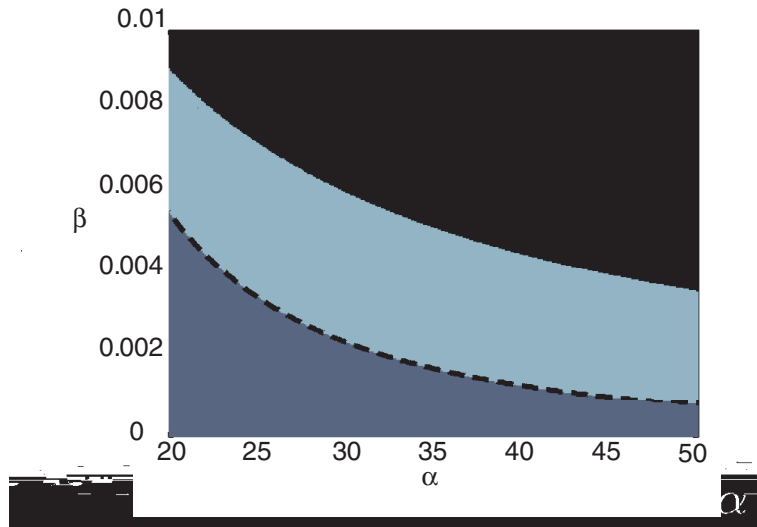


Fig. 2.5 Phase diagram in  $(\alpha, \beta)$  parameter space. Black denotes nonexistence of bumps; light grey denotes unstable bumps; dark grey denotes bumps that are stable with respect to perturbations associated with real eigenvalues. The dashed black line denotes location points where numerically stable bumps transition to traveling pulses. Other parameters are  $A = 0.001$ ,  $\tau = 1$ , and  $\sigma = 0.001$ .

enough synaptic depression (large  $\beta$ ) can destabilize a stationary bump that would be stable in the absence of depression.

**3. Two-dimensional bumps.** There have been few studies regarding the existence and stability of standing bumps in 2D neural fields [9, 15, 25, 29]. Laing and Troy [25] were the first to introduce partial differential equation (PDE) methods to study symmetry-breaking of rotationally symmetric bumps. Since then, PDE methods have been used to study the formation of multiple bump solutions, Turing patterns, traveling spots, and labyrinthine patterns in 2D neural fields with local negative feedback [9, 29]. In addition, standard stability analysis of stimulus-driven 2D neural fields with local linear negative feedback revealed symmetry-breaking breathers [15]. In all of these studies, the eigenmodes associated with instabilities were pure Fourier modes, which were straightforward to pick out using linear stability analysis. In our 2D neural field model, the rotationally nonsymmetric perturbations of bumps possess eigenmodes that are a mixture of pure Fourier modes. This makes the derivation of eigenvalues significantly more complex. Also, we must employ stability analysis techniques that heed the piecewise-smooth nature of the system. Thus, we now extend our analysis of stationary bumps in a 1D network to derive conditions for the existence and stability of radially symmetric stationary bump solutions of the corresponding 2D piecewise-smooth neural field model

$$(3.1a) \quad \frac{u(\mathbf{r}, t)}{t} = -u(\mathbf{r}, t) + \int_{\mathbb{R}^2} q(\mathbf{r}', t) w(|\mathbf{r} - \mathbf{r}'|) H(u(\mathbf{r}', t) - \theta) d\mathbf{r}',$$

$$(3.1b) \quad \frac{q(\mathbf{r}, t)}{t} = \frac{1 - q(\mathbf{r}, t)}{\tau} - q(\mathbf{r}, t) H(u(\mathbf{r}, t) - \theta),$$

where  $\mathbf{r} = (r, \theta) \in \mathbb{R}^2$  and

**3.1. Existence.** Consider a circularly symmetric bump solution of radius  $a$  such that  $u(\mathbf{r}, t) = U(r)$ ,  $q(\mathbf{r}, t) = Q(r)$  with  $U(a) = 1$ , and

$$\begin{aligned} U(r) &\geq 0 && \text{for } r \leq a, \\ (U(r), Q(r)) &\rightarrow (0, 1) && \text{as } r \rightarrow \infty. \end{aligned}$$

Imposing such constraints on a stationary solution of (3.1) gives

$$(3.2) \quad U(r) = \int_{\mathcal{U}} Q(r') w(|\mathbf{r} - \mathbf{r}'|) d\mathbf{r}',$$

$$(3.3) \quad Q(r) = (1 + \int_{\mathcal{U}} H(U(r) - U(r')) d\mathbf{r}')^{-1},$$

where  $\mathcal{U} = \{\mathbf{r} = (r, \theta) : r \leq a\}$  is the domain on which the bump is superthreshold. Substituting (3.3) back into (3.2) yields

$$(3.4) \quad (1 + \int_{\mathcal{U}} H(U(r) - U(r')) d\mathbf{r}') U(r) = \int_{\mathcal{U}} Q(r') w(|\mathbf{r} - \mathbf{r}'|) d\mathbf{r}',$$

where

$$(3.5) \quad \int_{\mathcal{U}} Q(r') w(|\mathbf{r} - \mathbf{r}'|) d\mathbf{r}' = \int_0^a \int_0^{2\pi} Q(r') w(\sqrt{r^2 + r'^2 - 2rr'\cos\theta}) r' dr' d\theta.$$

We can calculate the double integral in (3.5) using the Hankel transform and Bessel function identities, as in [14, 29]. Thus, we find that

$$(3.6) \quad \int_{\mathcal{U}} Q(r') w(|\mathbf{r} - \mathbf{r}'|) d\mathbf{r}' = 2 \int_0^a \hat{w}(s) J_0(sr) J_1(sa) s ds,$$

where  $\hat{w}(s)$  is the Hankel transform of  $w$ .

For the sake of illustration consider a Mexican hat weight distribution given by a combination of modified Bessel functions of the second kind [14, 26, 29]:

$$(3.7) \quad w(r) = \frac{2}{3} (K_0(r) - K_0(2r) - A(K_0(r/\lambda) - K_0(2r/\lambda))).$$

Such a weight function is qualitatively similar to a difference of exponential weight functions  $w(r) = (2\lambda)^{-1} (e^{-r} - Ae^{-r/\lambda})$ . Moreover, following previous studies of 2D neural field models [20, 25, 26, 29, 35], we can transform system (3.1) into a fourth-order PDE, which is computationally less expensive to evaluate. Using the fact that the corresponding Hankel transform of  $K_0(sr)$  is  $\mathcal{H}(s, r) = (s^2 + r^2)^{-1}$ , we have

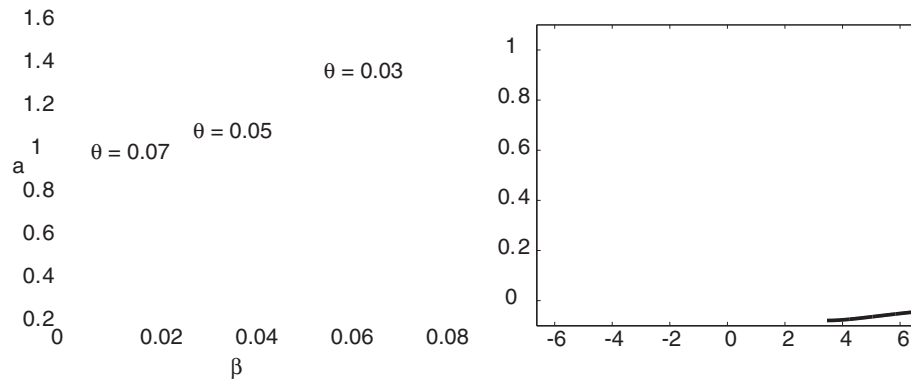
$$(3.8) \quad \hat{w}(s) = \frac{2}{3} (\mathcal{H}(s, 1) - \mathcal{H}(s, 2) - A(\mathcal{H}(s, 1/\lambda) - \mathcal{H}(s, 2/\lambda))).$$

Thus, the integral (3.6) can be evaluated explicitly by substituting (3.8) into (3.6) and using the identity

$$\int_0^{\infty} \frac{1}{s^2 + r^2} J_0(sr) J_1(sa) s ds \equiv \mathcal{I}(a, r, s) = \begin{cases} \frac{1}{s} I_1(sa) K_0(sr), & r > a, \\ \frac{1}{as^2} - \frac{1}{s} I_0(sr) K_1(sa), & r < a, \end{cases}$$

where  $I$  is the modified Bessel function of the first kind of order  $\nu$ . Thus, the stationary bump  $U(r)$  given by (3.4) has the form

$$(3.9) \quad U(r) = \frac{4a}{3(1 + \int_{\mathcal{U}} H(U(r) - U(r')) d\mathbf{r}')} (\mathcal{I}(a, r, 1) - \mathcal{I}(a, r, 2) - A(\mathcal{I}(a, r, 1/\lambda) - \mathcal{I}(a, r, 2/\lambda))).$$



If  $(r, t)$  denotes the perturbation of the circular bump boundary at polar coordinate  $(a, \theta)$ , then

$$u(a + r, t)$$



to lowest order in  $\epsilon$ . This leads to the following pair of equations:

$$(3.18) \quad \frac{\partial \psi(\mathbf{r}, t)}{\partial t} = -\psi(\mathbf{r}, t) + \psi(\mathbf{r}, t) + a \int_{\mathcal{A}_+(t)} (a, \mathbf{r}', t) w(|\mathbf{r} - \mathbf{r}'|) d\mathbf{r}' + \frac{a}{1 + \epsilon} \int_{\mathcal{A}_-(t)} (a, \mathbf{r}', t) w(|\mathbf{r} - \mathbf{r}'|) d\mathbf{r}',$$

$$(3.19) \quad \frac{\partial \psi(\mathbf{r}, t)}{\partial t} = -(\epsilon^{-1} + \epsilon) \psi(\mathbf{r}, t) - a \int_{\mathcal{A}_\#(t)} (a, \mathbf{r}', t) w(|\mathbf{r} - \mathbf{r}'|) d\mathbf{r}'.$$

Here

$$(3.20) \quad \epsilon^{-1} = |U'(a)| = \frac{2a}{1 + \epsilon} \int_0^\infty w(r) J_1(a/r) J_1(a) dr,$$

which, for the Mexican hat weight function (3.7), can be explicitly computed as

$$(3.21) \quad |U'(a)| = \frac{4a}{3(1 + \epsilon)} (I_1(a) K_1(a) - I_1(2a) K_1(2a) - A(I_1(a/r) K_1(a/r) - I_1(2a/r) K_1(2a/r))).$$

Equations (3.18) and (3.19) imply that the local stability of a stationary bump solution depends on solutions to a system of pseudolinear equations. As in the 1D case, we can obtain a class of solutions under the ansatz that the perturbation  $(a, \mathbf{r}, t)$  (equivalently,  $(\psi, t)$ ) does not switch sign at each  $\mathbf{r}$  for any time  $t$ . Thus, we assume (3.18) and (3.19) have separable solutions  $(\psi(\mathbf{r}, t), \psi(\mathbf{r}, t)) = e^{-t} (\psi(\mathbf{r}), \psi(\mathbf{r}))$ , where  $\psi$  is real and  $(\psi(\mathbf{r}), \psi(\mathbf{r}))$  are bounded continuous functions that decay to zero exponentially as  $|\mathbf{r}| \rightarrow \infty$ . Under this assumption, the domains  $\mathcal{A}_\pm$  are constant in time, so there is a common factor  $e^{-t}$  that cancels everywhere. In a similar u-6.6(t)-28(e) 13 1 H2757.7(t)2.2(he)-363.tio)dh

where we have simplified the argument of  $w(r)$  using

$$|(a, \theta) - (a, \theta')| = \sqrt{(a \sin \theta - a \sin \theta')^2 + (a \cos \theta - a \cos \theta')^2} = 2a \sin \frac{\theta - \theta'}{2}.$$



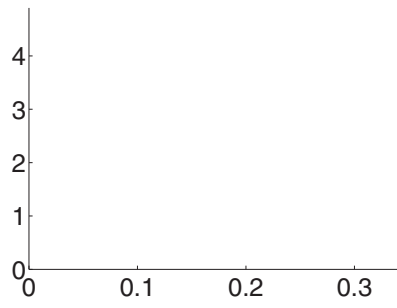






the lower positive branch of expansions) as the bump width approaches the value at which the upper and lower existence curves meet. As we show below (see Figure 3.4), the instability associated with positive real eigenvalues of the expansion perturbations









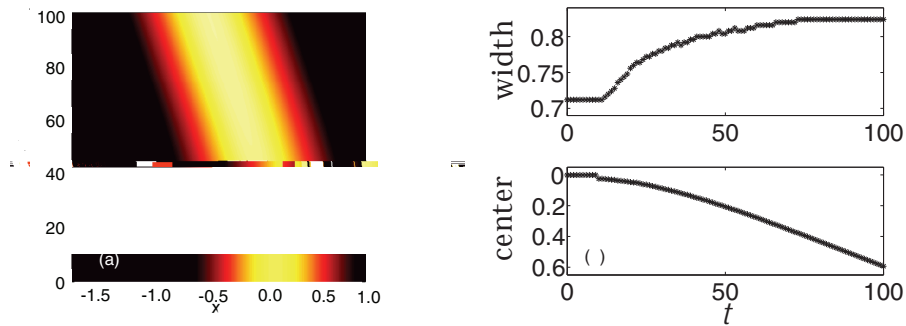


Fig. 4.1 Numerical simulation of a bump destabilized by a leftward shift perturbation. Plot of  $u(x,t)$  for an initial condition taken to be a stationary bump specified by  $u(x,0) = \exp(-x^2)$ . The solution is perturbed at  $t = 0$  by a leftward shift  $-x, t$  such that  $t = -x$  for  $t \in [0, 100]$  and zero otherwise. Bump width and center of mass plotted versus time. Bump width increases linearly following the perturbation, but eventually relaxes to a constant value as the solution evolves to a traveling pulse. The center of mass eventually moves linearly through space at the speed of the associated traveling pulse. Parameters are  $A = 1, B = 1, C = 1, D = 1, E = 1, F = 1, G = 1, H = 1, I = 1, J = 1, K = 1, L = 1, M = 1, N = 1, O = 1, P = 1, Q = 1, R = 1, S = 1, T = 1, U = 1, V = 1, W = 1, X = 1, Y = 1, Z = 1$ .

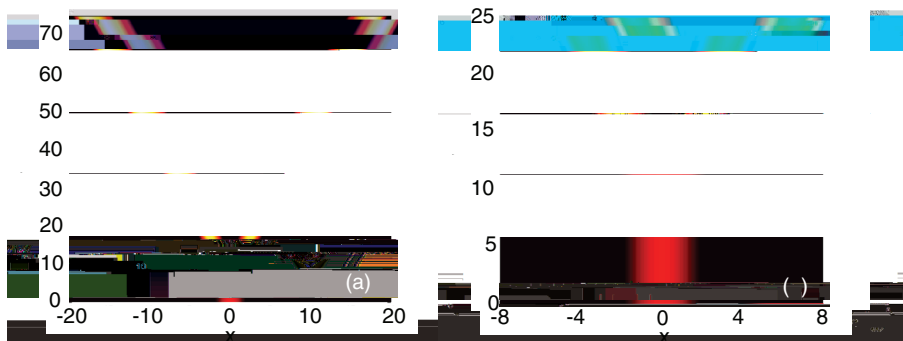


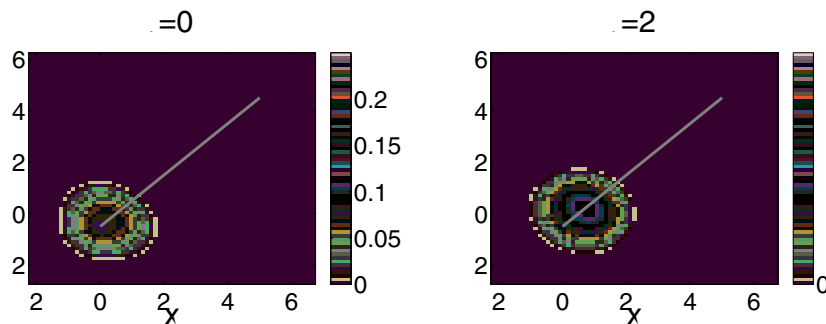
Fig. 4.2 Numerical simulation of a bump destabilized by an expanding perturbation. Plot of  $u(x,t)$  for an initial condition taken to be stationary bump specified by  $u(x,0) = \exp(-x^2)$ . The solution is perturbed at  $t = 0$  by an expansion  $+x, t$  such that  $t = x$  for  $t \in [0, 100]$  and zero otherwise. Plot of  $u(x,t)$  for  $t = 0$  to  $t = 70$ , showing initial expansion of the bump prior to splitting into two counterpropagating pulses. Parameters are  $A = 1, B = 1, C = 1, D = 1, E = 1, F = 1, G = 1, H = 1, I = 1, J = 1, K = 1, L = 1, M = 1, N = 1, O = 1, P = 1, Q = 1, R = 1, S = 1, T = 1, U = 1, V = 1, W = 1, X = 1, Y = 1, Z = 1$ .

When shift perturbations destabilize a bump, the resulting dynamics evolves to a traveling pulse solution. As we showed in previous work, synaptic depression is a reliable mechanism for generating traveling pulses in excitatory neural fields [19, 20]. As illustrated in Figure 4.1, following a perturbation by a leftward shift, the bump initially expands and then starts to propagate. Eventually, the traveling pulse’s width stabilizes to a constant value, larger than the initial bump width. The initial linear growth in the bump’s width is consistent with our linear stability calculations. In other simulations, we found that as synaptic depression strength is increased, the rate of linear growth in the width increases as well, which is also predicted by our stability analysis. In Figure 4.2, we show an example of how expansions destabilize the bump to result in two counterpropagating pulses. A closer look at the solution as a function of time immediately after the perturbation shows a transient phase,

where the superthreshold region is still a connected domain, prior to the splitting into two pulses. As also predicted by our stability analysis, we found that contraction perturbations did not drive the system to the homogeneous zero state, unless their amplitude was large enough to drive the system to the other side of the separatrix given by the smaller unstable bump (see Figure 2.1).

Next, to evolve the 2D system (3.1) in time, we use a fourth-order Runge–Kutta method with a  $200 \times 200$  spatial grid and a time-step of  $dt = 0.1$ . The integral term in (3.1a) is approximated using Simpson’s rule. We systematically examined whether taking finer grids changed stability results, and it does not. According to our stability analysis in the previous section, the dominant instability as  $\alpha$  is increased from zero is given by the shift perturbation. Thus, we explore this phenomenon at a point in parameter space where the bump is unstable to shifts (see Figure 3.4b). In Figure 4.3, we show the results of a simulation in which the initial condition was taken to be a bump solution given by (3.9) with a shift perturbation added. We find the solution evolves to a traveling spot similar to those seen in a previous study of a 2D neural field with spike frequency adaptation [9]. The solution evolves to have an invariant profile as it travels along a path in space, roughly indicated by a grey line in Figure 3.5. This is analogous to traveling pulse solutions in one dimension generated due to bump instabilities in one dimension shown in Figures 4.1 and 4.2.

**5. Discussion.** In this paper we analyzed the existence and stability of 1D and 2D stationary bumps in a piecewise-smooth neural field model with synaptic depression. We showed that the local stability of a bump is determined by solutions to







S. Coombes and M. R. Owen

- W. C. Troy and V. Shusterman *Patterns and features of families of traveling waves in large-scale neuronal networks*
- M. V. Tsodyks and H. Markram